Wave steepness from satellite altimetry for wave dynamics and climate studies

S. Badulin[1,2], V. Grigorieva[1], A. Gavrikov[1], V. Geogjaev[1,2], M. Krinitskiy[1], and M. Markina[1,3]

[1]Shirshov Institute of Oceanology, Russian Academy of Sciences, Moscow, Russia

[2]Laboratory of Nonlinear Wave Processes, Novosibirsk State University, Novosibirsk, Russia

[3]Lomonosov Moscow State University, Moscow, Russia

Abstract. Wave steepness is presented as an extension and a valuable add-on to the conventional set of sea state parameters retrieved from satellite altimetry data. Following physical model based on recent advances of weak turbulence theory wave steepness is estimated from directly measured spatial gradient of wave height. In this way the method works with altimetry trajectories rather than with point-wise data. Moreover, in contrast to widely used parametric models this approach provides us with instantaneous values of wave steepness and period. Relevance of single-track estimates of wave steepness (period) is shown for wave climate studies and confirmed by a simple probabilistic model. The approach is verified via comparison against buoy and satellite data including crossover points for standard 1 second data of Ku-band altimeters. High quality of the physical model

and robustness of the parametric ones are examined in terms of global wave statistics. Prospects and relevance of both approaches in the ocean wave climate studies are discussed.

1 Introduction

Sea waves is a complex physical phenomenon that affects (and is affected by) a number of processes in a wide range of spatial and temporal scales: from small-scale turbulence to large-scale ocean circulation. Wind waves which are driven mostly by local winds contribute to the ocean dynamics at relatively short scales of stormy regions while ocean swells transfer energy over thousands of miles [e.g. from the Roaring Forties to the Northern Pacific, see [*Snodgrass et al.,* 1966] and thus can be regarded as a large-scale process.

Conventional in situ measurements are not always relevant to the physical phenomenon of sea waves being essentially local, scarce in time and space, and not accurate enough [e.g. *Gulev and Grigorieva,* 2003]. In most cases this data provides two key wave parameters (sometimes, along with wind observations) for prediction and diagnosis of wind-wave coupling: signif-

icant wave height and wave period (mean, peak, zero-crossing etc.).

Remote sensing methods do not measure sea waves directly. Two general approaches are used to convert the measurable quantities into characteristics of sea state. Firstly, the conventional procedures of calibration and validation provide a basis for *empirical models of sea state from remote sensing data*. An alternative way relies upon essential physical links between the measured parameters and those being estimated. The latter approach leads to the development of *physical models of sea state* [*Badulin,* 2014]. These two approaches are widely used in satellite altimetry both individually and more often in a combination.

The model of electromagnetic scattering by a gaussian random sea surface provides a reference shape of the altimeter echo [*Brown,* 1977]. As the very first approximation the sea state parameters can be retrieved through fitting the measured echo to this shape [e.g. *Barrick and Lipa,* 1985]. The tangent of the leading edge of the echo is associated with significant wave height H_s: the sea is rougher, the edge is less steep. The normalized radar cross-section σ_0 is another parameter measured directly which is affected heavily by the sea surface roughness, sea spray from wave break-

ing, sea surface pollution etc. The latter makes H_s and σ_0 essentially correlated and constrains the application of the pair (H_s, σ_0) for empirical models of wind speed and wave period (see discussion in [*Badulin,* 2014]). This correlation can be regarded as a spurious one which effect is difficult to be controlled and evaluated.

Wave height H_s and its spatial gradient ∇H_s were suggested in the physical model by *Badulin,* [2014, *hereinafter* B14], as a new combination of measured parameters that leads to the following expression for the spectral peak period T_p [*Badulin,* 2014, equation 6]

$$T_p = 2^{1/5}\pi\alpha_{ss}^{-3/10}\sqrt{H_s/g}|\nabla H_s|^{-1/10}. \qquad (1)$$

The expression (1) does not refer to any empirical quantities but to the gravity acceleration g and the dimensionless physical parameter α_{ss} which is a direct equivalent of the fundamental Kolmogorov-Zakharov constant in the theory of wave turbulence [*Zakharov et al.,* 1992; *Badulin et al.,* 2007; *Badulin and Zakharov,* 2017]. It controls the essential physical link of the wave field where nonlinear transfer due to wave-wave interactions dominates over wind forcing and wave dissipation. For the growing wind sea it relates total wave energy

(wave height) to total wave input (spectral flux to/from waves). The value of α_{ss} has been evaluated numerically by *Badulin et al.,* [2008] and *Gagnaire-Renou, Benoit and Badulin,* [2011] and related to more than 20 experiments by *Badulin et al.* [2007]. The estimate $\alpha_{ss} = 0.67$ [*Gagnaire-Renou et al.*, 2011] is used in this study. Technically two crossover measurements of satellite altimeters are required for obtaining the vector module $|\nabla H_s|$ in (1) and thus for an accurate estimate of wave period. Fortunately, low exponent $1/10$ mitigates this requirement making the along-track measurements by a single altimeter acceptable in many cases of interest.

Being rewritten for μ the model [*Badulin,* 2014] provides a remarkably simple dependence on spatial gradient ∇H_s

$$\mu = \frac{\alpha_{ss}^{3/5}}{2^{2/5}} |\nabla H_s|^{1/5} \approx 0.596 |\nabla H_s|^{1/5} \qquad (2)$$

Here and after we refer to the steepness definition based on integral parameters of sea state, namely peak period

T_p and significant wave height H_s

$$\mu = \frac{\pi^2 H_s}{g T_p^2}.$$ (3)

The measured H_s and empirically estimated T_p in (3) can be essentially correlated while the alternative estimate (2) of wave steepness is free of any spurious correlations. The accuracy of the gradient ∇H_s measurements by altimetry can be improved with the modern technologies. Additionally, the gradient is less biased compared to wave height H_s itself because it is computed by subtracting two consecutive values which removes H_s systematic error. Thus, the passage to the tandem $(H_s, \nabla H_s)$ is seen as a conceptual step that introduces "a theoretical" wave steepness (2) into the conventional set of sea state parameters. This issue of prospective studies of sea waves has not been presented before in [*Badulin,* 2014]. Also the method itself has not been substantiated properly by comparison with in situ data. The paper is aimed to fill in this gap.

We begin with the discussion of the model [*Badulin,* 2014] in terms of the analogy with the model of geostrophic currents in order to specify advantages and disadvantages of the novel approach. The new method is

validated on Globwave satellite altimetry data (http://globwave.ifremer.fr). We demonstrate the correspondence of the results to the today's understanding of sea wave climatology [*Gulev and Grigorieva*, 2003] as well as "device-independent features" of the new approach. Global maps of wave steepness are presented and analyzed. Possible applications of the new approach in reconstructions of wind wave climate are discussed. The paper is summarized by the discussion of the prospects of the new method.

2 Two Models – One Principle for Satellite Altimetry

In this section we discuss two physical models of satellite altimetry both based on along-track gradients of parameters measured by altimeter.

2.1 Gradients of Sea Surface Height for Monitoring Geostrophic Currents

The well-known method of dynamical heights for large-scale currents (Figure 1, left) considers the geostrophic balance of the gravity and the Coriolis forces
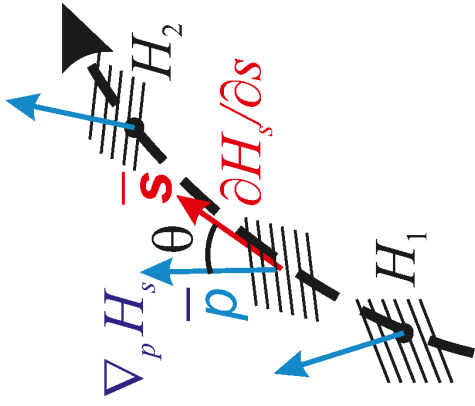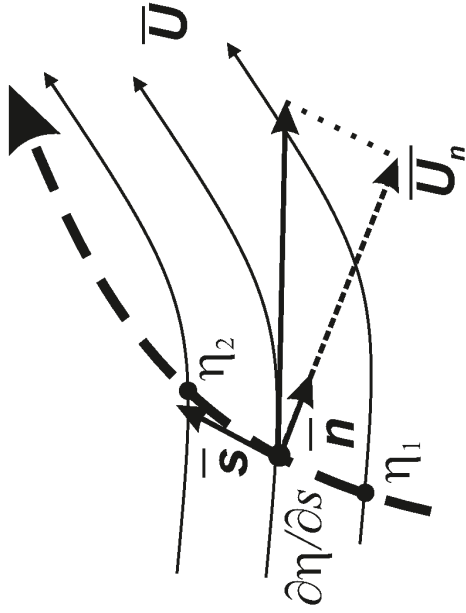
Figure 1. Left – setup of measurements of large-scale currents by satellite altimeter; right – setup of estimate of wave steepness from two consecutive along-track measurements of significant wave height by satellite altimeter. Different colors are used for along-track (red) and wave (blue) directions.

$$2\Omega\mathbf{Un}\sin\phi = -g\frac{\partial\eta}{\partial\mathbf{s}}\mathbf{s} \qquad (4)$$

where $2\Omega = f$ is the Coriolis parameter and ϕ is the latitude of the site of measurements. The general expression (4) says that the along-track derivative of the hydrodynamic pressure produced by variations of surface elevation η (g being gravity acceleration, the tangent unit vector $\mathbf{s}$) is balanced by the horizontal component of the current velocity $\mathbf{Un}$ which is normal to the track (the normal vector $\mathbf{n}$ in eq. (4). A single satellite track provides the only along-track component of the pressure field gradient (more specifically, sea surface elevation relatively to equipotential level) and hence a single component of the velocity $U_n = \mathbf{Un}$ in the cross-track direction. The full vector $\mathbf{U}$ can be derived from two intersecting tracks. Obviously, time interval between these two consecutive along-track measurements should be small enough.

Linearity of the basic relation (4) between measured (surface elevation η) and estimated (current velocity $\mathbf{U}$) values can be considered as a fortunate coincidence. In this case, the relationship between the errors in sea level measurements and the accuracy of geostrophic current estimates is very simple. Theoretically, the ac-

curacy of the estimates of geostrophic currents is limited by wavelength of the sounding pulse [*Dumont et al.*, 2011] that is approximately 2.2 cm for the Ku-band and 0.8 cm for the recently launched Ka-band altimeter SARAL/AltiKa. An additional advantage of this method comes from spatial scales of the phenomenon under study (large-scale currents) being large enough to reduce noise of altimeter data when averaged.

2.2 Gradients of Sea Wave Height for Wave Studies

Sea wave measurements require significantly shorter scales of averaging (both in time and space). The corresponding data is noisier and thus incomparably less accurate. However the accuracy of significant wave height measured by modern altimeters is better than 20 cm which is close to the accuracy of ocean buoys or better than one of visual observations [e.g. *Dumont et al.*, 2011].

Figure 1 illustrates a similarity of physical principles of altimetry measurements of large-scale currents (previous section and eq.(4) and wave steepness with the model [*Badulin,* 2014] (2). Measurements in two consecutive points give an estimate of the correspond-

ing directional derivative. For the geostrophic current this derivative is converted to the cross-track component of current velocity via linear relationship (4). A similar but heavily nonlinear conversion (2) of an unspecified projection of a spatial gradient gives a lower-bound estimate of wave steepness μ. The full vector ∇H_s and hence a "full" wave steepness μ can be obtained in crossover points of two altimeters. These cases are really rare because of the spatial and temporal requirements for mismatch in sea waves. Globwave database accepts mismatch of 30 minutes in time and 50 kilometers in space for the crossover points (http://globwave.ifremer.fr/products/globwave-satellite-data/satellite-crossovers) while spatial and temporal scale of wave field variability can be essentially shorter. The issue of physical scales becomes of key importance when considering the relevance of the method.

2.3 Physical Constraints for Altimetry Measurements of Sea State

A certain hierarchy of physical scales is implied for the model B14 validity. The realization of the method should respect this ranking in options of measurements, and data processing.

A characteristic wavelength λ (wave period T_p) is the shortest physical scale within the weakly nonlinear statistical description of water waves where the physical scale of wave-wave interactions obeys the well-known relationship [*Hasselmann*, 1962]

$$L_{nl} = \frac{1}{4\pi C_{nl}} \mu^{-4} \lambda. \qquad (5)$$

Even rather high steepness $\mu \simeq 0.1$ gives a large factor 10^4 in (5) that induces a long-lasted discussion on the relevance of statistical approach for wind-driven seas. In fact, the accurate estimate of the coefficient $C_{nl} \simeq 10^2$ in (5) reduces the scale of wave-wave interactions by two orders of magnitude [see *Zakharov and Badulin*, 2011 eqs.21,22]. For wavelength 50 meters and moderate $\mu = 0.05$ one has $L_{nl} = 6.36$ km which is a reasonable value for the theory to be valid.

Similar estimates of scales of wind wave growth from existing parametric models [e.g. *Cavaleri et al.*, 2007] generally leads to the following relationship

$$L_{\text{wind}} \sim \frac{\rho_w}{\rho_a} \frac{\lambda}{4\pi} \frac{1}{C_{\text{wind}} \left(\omega/\omega_0 - 1\right)^n} \qquad (6)$$

with large ratio ρ_w/ρ_a (ρ_w and ρ_a are water and air densities) and relatively small dimensionless coefficient

$C_{\text{wind}} \simeq 0.1$. Characteristic frequency ω_0 is usually associated with spectral peak and the exponent $1 \leq n \leq 2$. For wave input parameterization by [*Donelan and Pierson*, 1987] $C_{\text{wind}} = 0.194$, $n = 2$, the same wavelength $\lambda = 50$ m and inverse wave age $\omega/\omega_0 = 2$ one has $L_{\text{wind}} = 16$ km. More conservative wave input function by [*Hsiao and Shemdin*, 1983] ($C_{\text{wind}} = 0.12$) gives $L_{\text{wind}} \approx 25.5$ km. The quantitative comparison of L_{nl} and L_{wind} leads to a key realization: wind wave growth occurs at scales which are, typically, longer (or even much longer) than scales of nonlinear relaxation of water waves (see Figure 3 in [*Zakharov and Badulin,* 2011]). It justifies validity of the asymptotic theory of wave growth [*Badulin et al.*, 2007; *Zakharov*, 2010] when

$$L_{nl} \ll L_{\text{wind}}. \tag{7}$$

The satellite altimetry assumes a sufficiently large footprint L_a of few kilometers. To be consistent with the statistical description of sea wave field L_a should be close or larger than the scale of the wave field relaxation associated with the fastest physical mechanism of wave-wave interactions, i.e.

$$L_a \geq L_{nl}.$$

A new physical scale ΔL appears when computing spatial gradient of wave height H_s between two consecutive footprints. This scale should be close to or larger than the footprint size L_a to ensure independence of two consecutive measurements. On the other hand, ΔL should be less (much less) than the scale of wave field variations associated with wind input and dissipation. Finally, we come to the following sequence of physical scales (cf. B14, eq.11)

$$L_{nl} \leq L_a \leq \Delta L \ll L_{\text{wind}} \qquad (8)$$

In practice, the formal requirement "much less" ($\ll$) at the very end of the sequence (8) can be replaced by a more flexible condition of simple inequality but the gap between two key physical scales of sea state, L_{nl} and L_{wind}, should exist and scales of altimeter measurements, L_a and ΔL, should fall into this gap for the method to work. The critical point of conditions (8) is an essential dependence of the scales involved on sea state and first of all on wavelength λ and wave steepness μ (H_s and T_p). As shown in this paper (see also B14 the standard 1 second data assimilated in the databases of Ku-band satellite altimetry (e.g. Globwave) are likely relevant to the scaling (8) for wind-driven seas and thus can be used for estimating wave

steepness and wave period. Long and smooth waves ($\mu \lesssim 0.03$) does not meet the requirements of the method and their steepness cannot be assessed with the method discussed. Thus, our approach being selective in physical scales can filter off particular features of sea state making "visible" only a fraction of the wind-driven seas. This point should be taken into account in areas where wind waves co-exist with pronounced swell, the so-called "swell pools" [*Chen et al.*, 2012].

Our experiments with high rate altimetry data (20 Hz, SGDR – Sensor Geophysical Data Record format) have not shown essential difference in estimates of wave steepness and period corresponding to spatial averaging in a range 3–15 km. Strictly speaking, the averaging of 20 Hz data in time is not correct because of nonlinearity of dependence of the estimated wave height H_s on the altimeter pulse shape. In order to solve this issue proper analysis of individual waveforms (for Envisat RA-2 1800 Hz) is required which is out of the scope of the current study.

The parametric models of sea state from altimetry data operating with one-point measurements [e.g. *Gommenginger et al.*, 2003; *Mackay et al.*, 2008] of H_s and σ_0 are formally free of the restrictions like those of the physical model B14. But inherent spu-

rious correlation of the measured characteristics bind the performance of a parametric approach when using two-parametric (multi-parametric) dependency. In case of the pair (H_s, σ_0) the anticorrelation has a physical explanation: higher waves provoke more frequent breaking and, thus, lower reflection from the sea surface (lower σ_0). Implicit limitations and drawbacks of parametric approaches will be discussed below for the model by *Gommenginger et al.*, [2003, hereinafter G03].

In fact, *the parametric models represent the best fit of estimates* to in situ buoy measurements. Therefore, these models provide a sort of climatological approximation "killing" an essential variability of the wave steepness and period. On the contrary instantaneously measured H_s, ∇H_s in *the physical model* B14 *preserve the natural variability of estimated parameters*.

The above physical model scaling considers an idealized case of wave development in a stationary spatially homogeneous sea while a number of physical effects can limit or even cancel the model validity in the real ocean. The effect of large-scale current on wind waves can be evaluated within the geometric optics approach [*Voronovich*, 1976]. The large-scale current gradient $\nabla\mathbf{U}$ forces waves to change their length (wave period) and amplitude. For small variations the relationship is

quite simple

$$\frac{|\nabla H_s|}{H_s} \simeq \frac{|\nabla \mathbf{U}|}{C} \qquad (9)$$

with $C = g/\omega$ being wave phase speed. Similar estimate of wave height gradient in the model (2) gives

$$\frac{\nabla H_s}{H_s} \approx 3.33 \frac{\omega}{C} \mu^4 \qquad (10)$$

In order to separate wind and current effects the dimensionless values $|\nabla \mathbf{U}|/\omega$ and μ^4 should be compared. For $|\nabla \mathbf{U}| = 10^{-6} \mathrm{s}^{-1}$ (1 m/s per 1000 km) and $\omega = 0.3$ s^{-1} (≈ 30 meters wavelength) the critical steepness is $\mu_{\mathrm{crit}} \approx 0.03$ that corresponds to rather smooth swell sea. Higher gradient $|\nabla \mathbf{U}| = 10^{-5} \mathrm{s}^{-1}$ (1m/s per 100 km) observed in the areas with intensive currents results in the value $\mu_{\mathrm{crit}} \approx 0.056$ which makes the model (2) still applicable in this case.

The problems multiply with the complexity of estimates of wave steepness for the seaside region. To validate the B14 model in the near-shore area, one must consider a number of physical processes (and corresponding scales) that affect wave evolution. What is more, the proximity of the coastline implies special corrections for altimeter standard products [*Vignudelli et*

al., 2011]. This research focuses on the global climatology of sea waves, therefore, method validation is carried out under open sea conditions (farther than 50 km to the shoreline).

3 Two Approaches for Wave Studies in Altimetry Data

In this section the features of the parametric and physical approaches are demonstrated for Globwave data [see also *Gavrikov et al.*, 2016] via comparison with buoy data and crossovers from different altimeters.

3.1 Satellite/Buoy Match-ups. Validity Test for the Pair $(H_s, \nabla H_s)$

The Globwave database of match-ups accepts buoy and altimeter measurements within the 60 km and 60 minute span. In order to meet the requirements of the physical constraints stated in section 2.3. *Physical constraints for altimetry measurements of sea state,* a more rigorous quality control was applied. Match-up distance has been reduced to 30 km and the time mismatch of buoy and satellite measurements — to

30 minutes. Only the altimetry data with quality flags "good" in three consecutive points were used for computation of along-track components of the gradient ∇H_s. The described constraints have reduced the number of analysed Envisat records to 155 in 2011.

Figure 2 demonstrates results of the comparison of wave parameters from NDBC and Envisat data. Figure 2a shows a good agreement for SWH. Mean-over-spectrum wave periods retrieved by the G03 model give an expected correspondence with NDBC measurements (Figure 2b). The root-mean-square deviation of the estimates does not exceed 1 second. Similar scatterplot of the wave period with the B14 model (Figure 2c) demonstrates a larger dispersion. Nevertheless this dispersion cannot be regarded as the model error only: comparison of wave periods provided by G03 and B14 in Figure 2d demonstrates good correspondence of the two models based on essentially different principles. Note, that the parametric model G03 (Figure 2b) operates with the mean-over-spectrum period T_m while the B14 model (2) refers to the spectral peak period T_p, which in general exceeds T_m by 10–20% [*Babanin and Soloviev,* 1998].
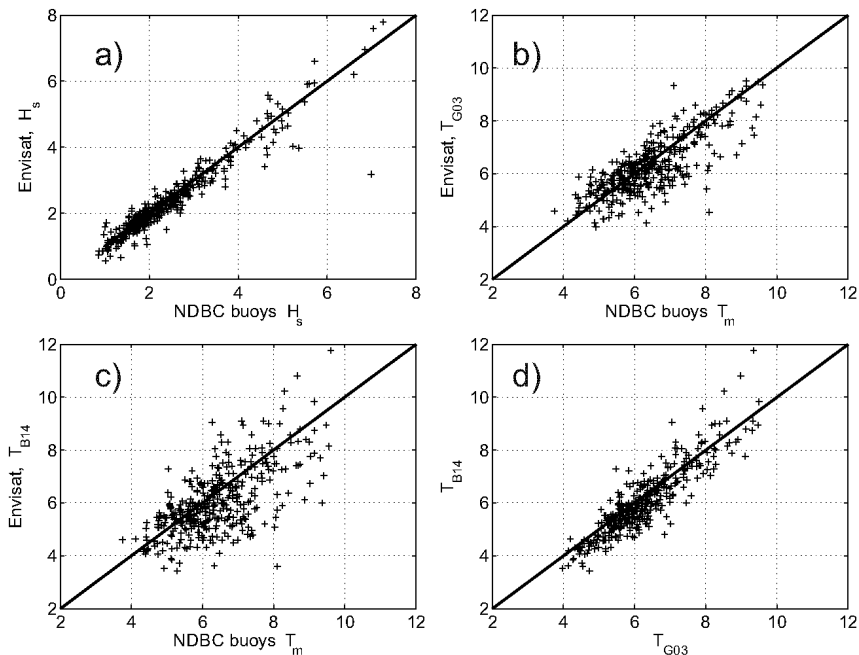
Figure 2. Scatter diagrams for altimeter (Envisat, 2011) and in situ NDBC buoys measurements for the Glob-wave database of match-ups. a) – significant wave heights (SWH); b) – mean-over-spectrum wave periods T_m measured by buoys (abscissa) and altimeter (ordinate) estimated by the parametric model G03; c) – mean-over-spectrum wave periods T_m measured by buoys (abscissa) and altimeter (ordinate) estimated by the physical model B14; d) – wave periods of G03 vs those of B14 model.

3.2 Satellite Crossovers. Full-gradient and Single-track Estimates of Wave Steepness and Periods

Altimeter crossovers are computed for pairs of satellites in order to provide a comprehensive dataset of coincident measurements that can be used to monitor the quality of each sensor and improve their calibration. In the context of the model B14 this data enables to evaluate a full gradient ∇H_s as a vector sum of two single-track estimates and thus to get a "full" (not a single-track) estimate of wave steepness (2) and period T_p (1). We set the mismatch of satellite measurements to be $r_c = 5$ km in space and $t_c = 900$ s in time in order to meet physical constraints discussed in the above sections. The assumed characteristic scales of wave field homogeneity and stationarity r_c, t_c are determined by a simple relationship $r_c = t_c \times C_{\text{waves}}$ where a characteristic speed $C_{\text{waves}} \approx 5.6$ m·s^{-1} corresponds to the group velocity of deep water waves with period $T_p \approx 7.2$ s (wavelength $\lambda \approx 75$ meters). This restriction along with quality flags "good" for three consecutive measurements near a crossover point gives 653 records for the pair Envisat-Jason-1 for the year 2011 for latitudes $60°$S – $60°$N.

Figure 3a,b show a good agreement for the conven-
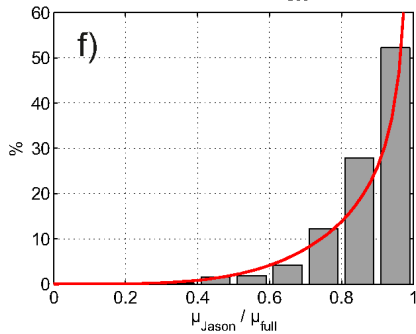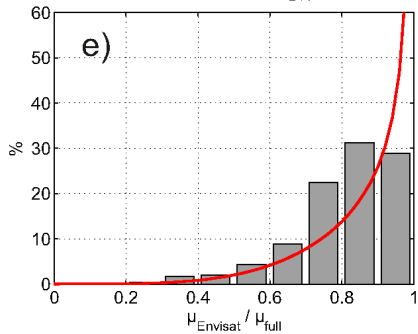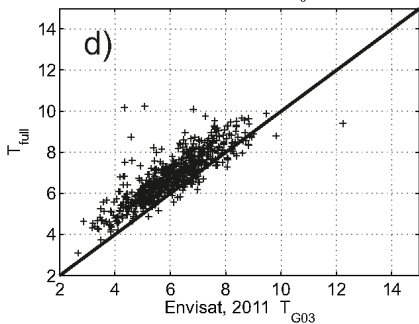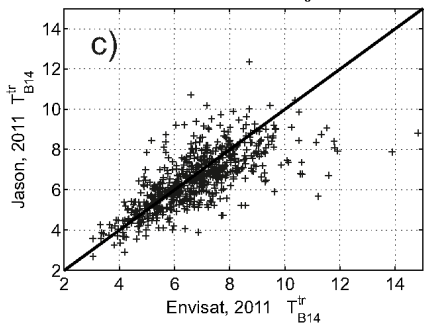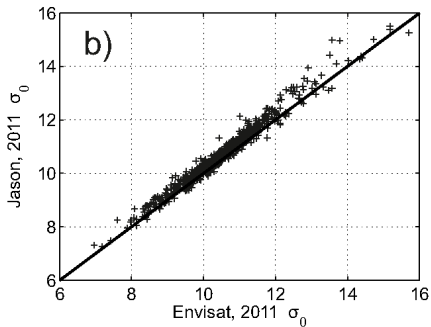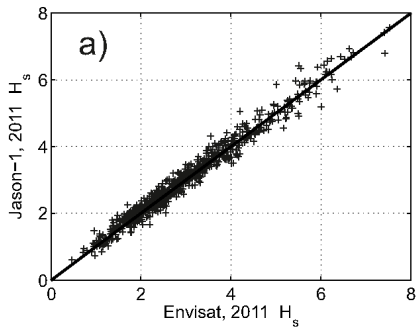
**Figure 3.** Measurements of Jason-1 and Envisat for the year 2011, totally 653 in cross-over points. Scatter diagrams for a) – significant wave height; b) – normalized radar cross-section; c) – single-track estimates of wave periods by the model B14; d) – "full" estimate of wave period T_{B14}^{full} vs mean-over spectrum wave period T_{G03} of the model G03 in crossover points; e, f) – histograms of the ratio μ_{tr}/μ_{full} (single-track to the full-gradient estimates) for Envisat (left) and Jason-1 (right) in crossover points. Solid line shows distribution for the probabilistic model (12) of the measured single-track μ_{track} with evenly distributed angles between satellite track and wave height spatial gradient ∇H_s.

tional pair (H_s, σ_0) measured with different altimeters. Single-track estimates of wave periods by Envisat and Jason-1 with the model B14 also demonstrate a reasonable correspondence (Figure 3c). Full gradient ∇H_s assessment in crossover points again gives remarkably good consistence of models of wave period G03 and B14 (Figure 2d). The "full" peak period T_p from the B14 model appears to be approximately 15% higher than the mean wave period of G03 in full agreement with the remarks of the previous paragraph and findings of [*Babanin and Soloviev*, 1998].

The bottom row presents probability density functions (hereinafter PDF) of the ratio μ_{track}/μ_{full} of single-

track μ_{track} and "full" μ_{full} wave steepness for Envisat (Figure 3e) and Jason-1 (Figure 3f). According to (2) the ratio $s = \mu_{\text{track}}/\mu_{\text{full}}$ is proportional to $(\cos\theta)^{1/5}$ (θ is angle between gradient ∇H_s and track direction, see right Figure 1 and cannot be greater than 1. We also assume $0 \leq \theta \leq \pi/2$ because of modulo in (2) and evenness of cosine function. Probability $p_\theta(\theta)$ for angle θ can be easily converted into dependence on this directional factor s:

$$p_s(s) = p_\theta(\theta(s)) \left| \frac{d\theta}{ds} \right| = p_\theta(\theta(s)) \frac{5s^4}{\sqrt{1 - s^{10}}} \qquad (11)$$

The uniform (equiprobable) distribution $p_\theta(\theta) = 2/\pi$ (PDF is normalized by $\int_0^{\pi/2} p_\theta(\theta)d\theta = 1$) recasted into $p_s(s) \equiv p_s(\mu_{\text{tr}}/\mu_{\text{full}})$ is shown in Figure 3e,f by solid lines. It demonstrates quite close correspondence with histograms for both Jason-1 and Envisat distributions. Theoretical p_s (see (11) gives probability 85% of the ratio $\mu_{\text{track}}/\mu_{\text{full}}$ to be 0.75 or higher, i.e. 85% of single-track measurements underestimate "full" magnitude of wave steepness μ_{full} by less than 25%. An alternative characteristics of quality of single-track measurements of wave steepness can be given in terms of probabilistic mean

$$\langle s \rangle = \left\langle \frac{\mu_{\text{tr}}}{\mu_{vfull}} \right\rangle = \int_0^1 s p_s(s) \frac{5s^4 ds}{\sqrt{1 - s^{10}}} \qquad (12)$$

For uniform distribution $p_\theta = 2/\pi$ one has $\langle s \rangle \approx$ 0.88 that makes the single-track estimates acceptable in many cases of interest, say, for global mapping of wave steepness.

The difference between two missions in histograms can be easily explained by domination of zonal circulation over the meridional. As a result, the polar orbit of Envisat (orbit inclination $98.6°$) exhibits more anisotropic effect of the wind field as compared to Jason-1 (orbit inclination $66°$). In this way the particular features of satellite missions (e.g. orbit inclination) can reduce the accuracy of the single-track estimates of global steepness.

Nevertheless the single-track estimates provide rather good reference for the "full" wave steepness and wave period. These estimates can be used as an extension of conventional altimetry of sea state parameters particularly in the context of wave climatology.

3.3 Gradient Measurements for Studies of Wave Dynamics

As indicated above two models of wave period based on quite different physical principles demonstrate a quantitative agreement. In this regard the new approach with the pair $(H_s, \nabla H_s)$ looks an unreasonable complicacy because of computations of spatial gradients ∇H_s that potentially leads to the loss of accuracy. The strongest argument for the novel approach is in additional information provided by along-track variations of the measured parameters. The structured records allow for tracking wave dynamics, thus, extending "static" wave parameters of point-wise data collections.

Figure 4 presents PDFs of wave parameters with pairs (H_s, σ_0) (left column) and $(H_s, \nabla H_s)$ (right) for three altimetry missions: ERS-2 (1995–2011), Envisat (2002–2012) and Jason-1 (2001–2013) for 2007 when all of them were operating. Only data with quality flags "good" for latitudes $60°\text{S} - 60°\text{N}$ have been considered. Measurements of ERS-2 are absent in the Southern hemisphere during 2007. Estimates for year 1998 with full coverage did not show a visible difference in wave steepness probability for the Southern and Northern hemispheres. While all altimeters provide quite
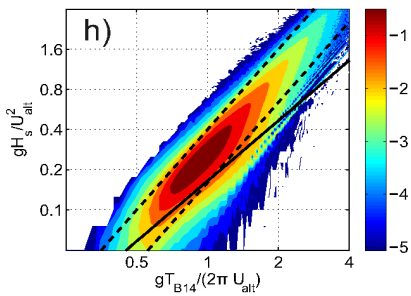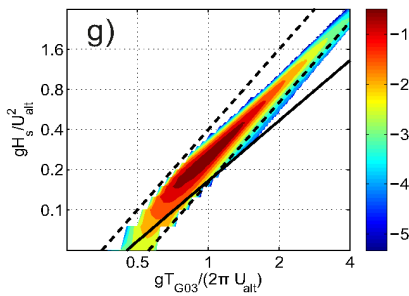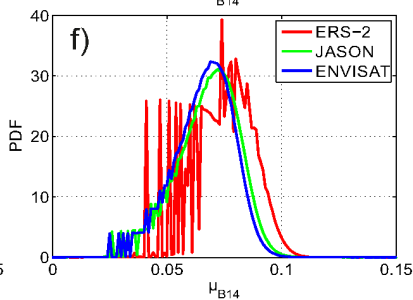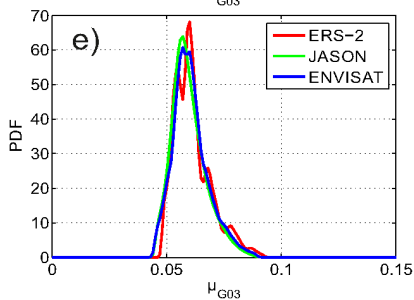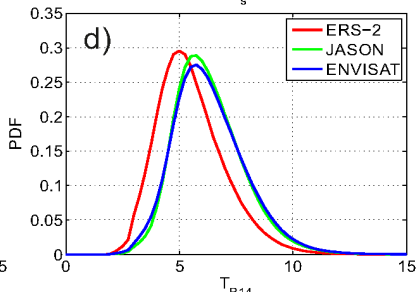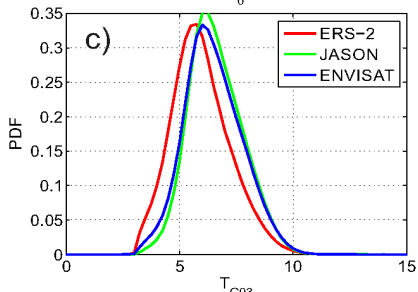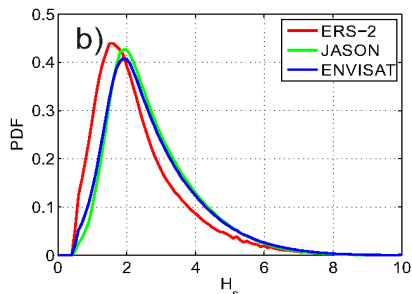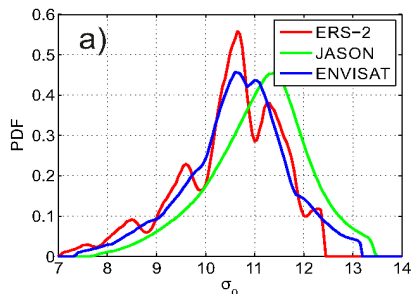
Figure 4. PDFs for a) – normalized radar cross-section σ_0; b) – significant wave height H_s; c) – wave period T_{G03} for the model G03; d) – wave period T_{B14} for the model B14; e) – wave steepness for the model G03; f) – wave steepness for the model B14; g) – dimensionless wave height gH_s/U_{alt}^2) vs wave age $gT_{G03}/(2\pi U_{\mathrm{alt}})$ for the model G03; h) – dimensionless wave height gH_s/U_{alt}^2) vs wave age $gT_{B14}/(2\pi U_{\mathrm{alt}})$ for the model B14.

close smooth PDFs for H_s (Figure 4b) the PDFs of the normalized radar cross-section σ_0 (Figure 4a) show a number of problems. The ERS-2 distribution (red curve) has pronounced peaks which look like artifacts due to inaccurate data processing. The Envisat curve (blue) can be seen as a smoothed approximation of the ERS-2 PDF but it still has twin-peak peculiarity near the distribution extremes. The Jason-1 dramatically differs from the two cases being smoother and with a single maximum shifted to higher σ_0.

Calibration/validation procedures (individual for each altimeter) does not reveal this evident shortcoming of retrieval σ_0 from altimeter pulses when being used for parameterization of wave periods and near-surface wind. In Figure 4c the distribution of wave periods estimated with the σ_0-based G03 model looks quite regular: pronounced oscillations of the σ_0 PDF in Figure 4a disap-

pear. Possible explanation of this effect can be found in a strong correlation of H_s and σ_0: their combination $\sigma^0 H_s^2$ in the resulting expression for wave period [eq.4 in *Gommenginger et al.*, 2003, σ^0 – the normalized radar cross-section in the authentic non-dB form] compensates the oscillations. While these peaks disappear in PDF of wave period they still remain visible for wave steepness of ERS-2 in Figure 4e.

The pair $(H_s, \nabla H_s)$ provides smooth patterns for estimates of wave periods (Figure 4d) with a lag of the ERS-2 curve and, what is more important, with essentially wider distributions in comparison with the G03 estimates (Figure 4c). The distribution for wave steepness in Figure 4f reveals another issue which is a high noise of wave height gradient. It makes estimates of wave steepness from the ERS-2 data useless while those of wave period remain acceptable because of lower exponent $1/10$ in (1).

Comparison of the wave steepness distributions shows qualitative disagreement of the conventional pair (H_s, σ_0) and the new one $(H_s, \nabla H_s)$ (Figure 4e,f). In both cases distributions are localized in approximately the same range $0.05 < \mu < 0.1$ but the "conventional" estimate (Figure 4e) gives sharper patterns (note different scales of ordinates in the panels). Similar sharpening of

PDF for the G03 model can be seen for wave periods (cf. Figure 4c,d). This qualitative dissimilarity of probabilistic features of B14 and G03 (and more generally disagreement between physical and parametric models) reflects conceptual difference of the pairs of measured quantities (H_s, ∇H_s) or (H_s, σ_0). As noted above (see sect.2.3 the physical model B14 *directly assesses instantaneous values* based on explicit physical assumptions while *its parametric counterpart* G03 *is looking for the best fit* to reference data (e.g. ocean buoys) of an inherently probabilistic dependence on (H_s, σ_0). In other words, a parametric approach targets to the most probable estimates rather than the instantaneous values.

Strong argument for improved relevance of the B14 approach can be found in distributions of dimensionless wave height and period scaled by wind speed. Figure 4g,h demonstrate dramatic discrepancy of two approaches in their ability to reflect sea wave dynamics. PDF is plotted for dimensionless wave period $\tilde{T} = gT_p/(2\pi U_{\mathrm{alt}})$ (wave age) and dimensionless wave height $\tilde{H} = gH_s/U_{\mathrm{alt}}^2$. The similar approach based on physical scale of wind speed [*Kitaigorodskii*, 1962] is widely used in sea wave studies [e.g. *Hwang et al.*, 1998; *Cavaleri et al.*, 2007]. It provides a ground for quantitative predictions like the *Toba* [1972] 3/2 law, 5/3

law of *Hasselmann et al.* [1976], 4/3 power-law dependence of *Zakharov and Zaslavskii* [1983] or one of fully developed sea [*Pierson and Moskowitz*, 1964]. These models demonstrate both an effectiveness and a deficiency of the wind speed scaling: a large scatter of experimental data is observed using dimensionless $\tilde{T}$ and $\tilde{H}$ [e.g. *Donelan et al.*, 1992; *Abdalla and Cavaleri*, 2002; *Hwang and Wang,* 2004]. The scatter reflects a non-universality of wind-wave coupling when features of wind over waves (gustiness, stratification etc.) affect the wave growth.

The existing non-universality or in other words diversity of wave dynamics in terms of dimensionless $\tilde{T}$ and $\tilde{H}$ is seen when following the B14 approach (Figure 4h). Power-law dependencies corresponding to the *Toba* [1972] 3/2 law (solid line) and to constant values of wave steepness $\mu = 0.1$ and $\mu = 0.04$ (dashed) are given for reference in Figure 4h. The distribution pattern covers both cases of rough sea ($\mu \approx 0.1$) and of the mature wind sea of *Pierson and Moskowitz* [1964] ($\mu \approx 0.04$). The shrinking of the G03 distribution can be treated as a corruption of wave physics that implies rather wide dispersion of the PDF due to diversity of effects of wave growth. The derivation itself of the parametric model [see sect.3 in *Gommenginger et al.*, 2003]

postulates the proximity to a constant wave steepness. This is not consistent with the dynamical laws predicting a decrease of wave steepness with growing wave age. Alternatively, a remarkable spreading of the B14 PDF to high wave ages matching the line of the Toba law can be treated as a manifestation of the effect of nonlinear transfer to low frequencies [*Glazman*, 1990].

3.4 Global Distributions of Wave Steepness: A Snapshot

High quality of altimetry measurements of wave height H_s and near-surface wind speed U_{alt} has been demonstrated in many studies [e.g. *Young et al.,* 2011]. Recently good agreement has been found between global distributions of wave periods retrieved from altimetry data and Voluntary Observing Ship data (VOS) [*Gavrikov et al.,* 2016; *Grigorieva and Badulin,* 2016]. It provides us with a ground for incorporating the altimetry data into conventional climatology of sea waves [*Gulev and Grigorieva,* 2003]. In general this climatology operates with mean values averaged both in space (in coordinate boxes) and time (monthly, annually). The geographical distributions of mean wave heights and periods appear quite representative and useful for further analysis in the context of climate changes [*Gulev et al.,*

2003; *Gulev and Grigorieva,* 2006] and wave extremes [*Grigorieva and Gulev,* 2008]. Similar global mapping of wave steepness looks questionable because the latter varies in an incomparably narrower range than wave heights or periods.

Figure 5 shows a geographical distribution of wave steepness in 2011 averaged over boxes $2° \times 2°$ for Envisat data. Wave steepness has been estimated with the model B14 (eq.(2) and top of Figure 5 and the parametric model G03 (bottom Figure 5 with μ defined by (3). Both maps show similar general patterns with pronounced latitudinal dependence and maxima in the Southern and Northern Atlantic and Pacific Ocean. Along with systematic underestimation of wave steepness by G03 we can also see discrepancies in particular enclosed basins (Mediterranean, Mexican Gulf etc.) and marginal seas (e.g. Indonesian seas).

Figure 5 provides a very preliminary look at *wave steepness climatology*. Relatively low variability (within few percents of typical magnitude) does not reflect a crucial role of this physical parameter in wave dynamics. In fact such key wave parameters as energy and momentum fluxes are heavily nonlinear functions of wave steepness.

Figure 6 demonstrates the key message of the above
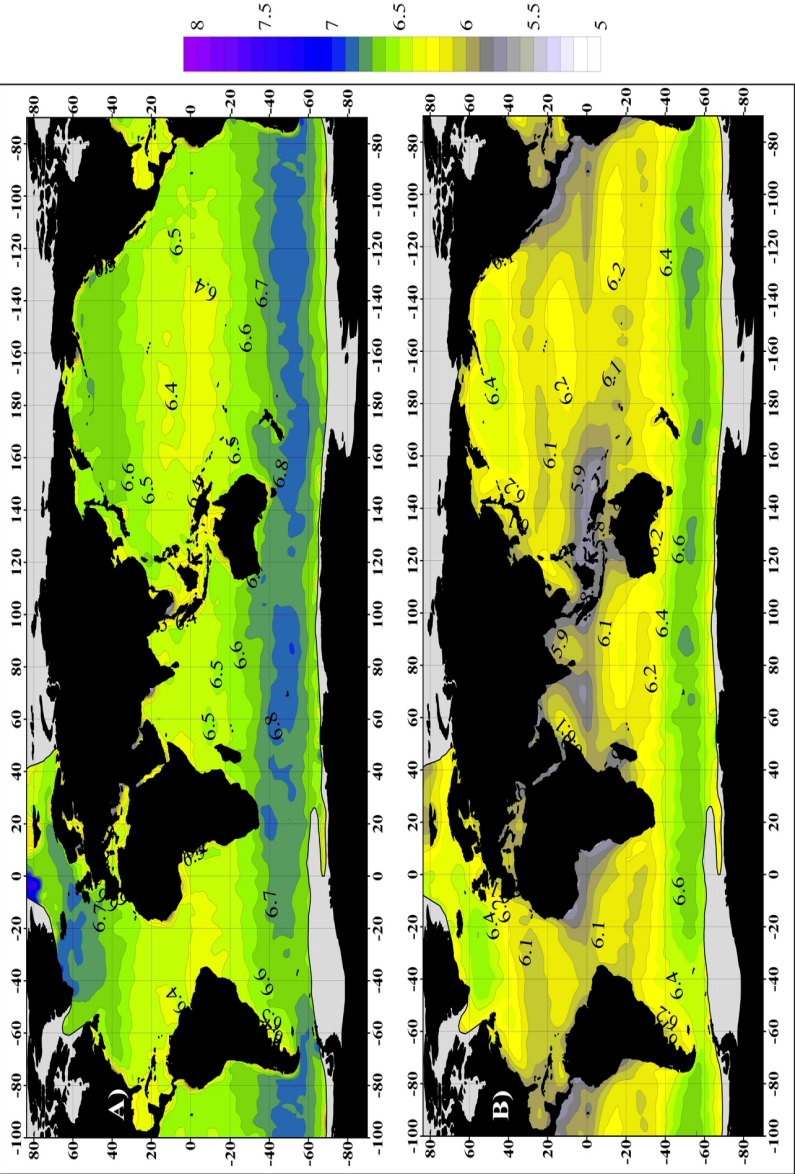
Figure 5. Global distribution of wave steepness derived from Envisat data in 2011. Top – physical model B14; bottom – parametric approach G03. Wave steepness values are multiplied by 100.

sections on the effect of specific approach (parametric or physical) on climatological constructions. Probability density functions are presented for the authentic data set (Envisat, 2011) of wave steepness (left panel) and for values averaged over $2° \times 2°$ coordinate boxes (right panel). In Figure 6a the physical model B14 (grey) gives a rather wide distribution of the authentic data (as expected from Figure 4f,h while the parametric approach G03 contracts the values in a narrow range 0.05–0.08 (black). The physical approach at least doubles this range and thereby reflects an essentially wider variability of *the instantaneous wave steepness*. The parametric model G03 in turn exhibits relatively weak dispersion of *the most probable wave steepness.*

The distributions of mean values of wave steepness, averaged over coordinate boxes $2° \times 2°$ in Figure 6b, look remarkably different for the models G03 and B14 (cf. Figure 6a,b). The dispersion of the first one (G03) remains roughly the same for authentic data while the width of the sampling B14 distribution squeezes by a factor $\sqrt{N_{2\times 2}}$ ($N_{2\times 2}$ being the number of data in $2° \times 2°$ coordinate box, $N_{2\times 2} \approx 100 - 400$ in our example). Such squeezing of the mean value distribution indicates that the sets of the steepness, evaluated within B14 in each $2° \times 2°$ box, are the realizations of essentially the
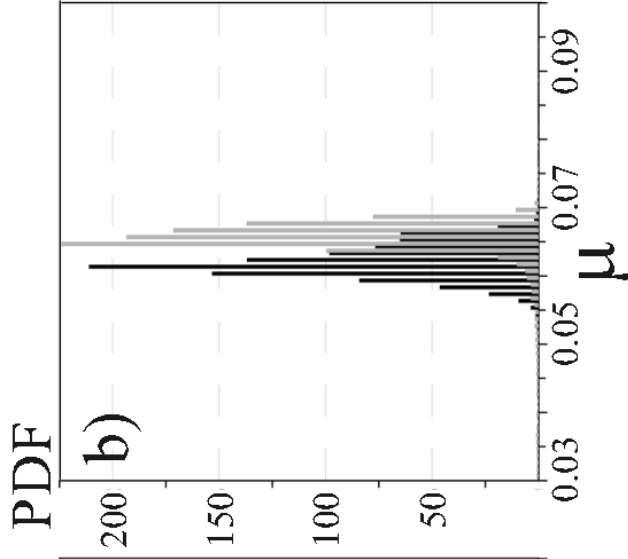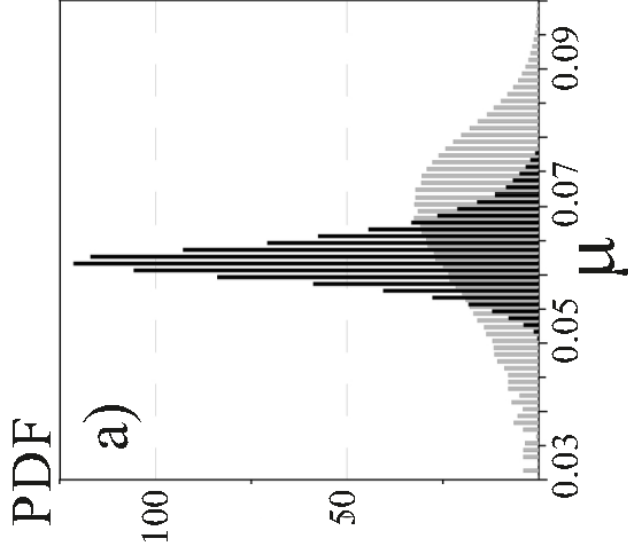
Figure 6. Probability density functions (PDF) for wave steepness estimates made within the parametric model G03 and the physical one by B14. a) – PDF for individual estimates of wave steepness; b) – PDF for the set of $2° \times 2°$ averaged wave steepness.

same random process. However, the best-fit model G03 does not reveal such universality.

This result suggests quite surprising climatological interpretation:

Climatology of wave steepness is quite indifferent to the geographical region in contrast to wave height H_s and period T_p that demonstrate significant regional variations.

In this way an incorporating wave steepness into today "classic" wave climatology requires more subtle methods of data analysis. The found universality of wave steepness climate within the B14 model does not mean a universality of wave dynamics in space and time. A thorough analysis of the global wave steepness distributions with two fundamentally different methods allows us to broaden our understanding of the wave dynamics.

4 Discussions

Satellite altimetry is a valuable source of data for ocean studies. The applications of this data are broad-ranging though measurements of sea surface elevation remain the primary goal of the today altimetry. These mea-

surements provide an input for assessments of large-scale dynamics of the ocean where sea level variations are considered as a driver of ocean currents together with the Coriolis force. In this way the field of the variations, i.e. spatial gradients of sea level are analyzed and processed.

Recent progress in remote sensing technologies allows measurements of sea wave height and hence its along-track variations. Potentially these records contain information on along-track wave dynamics but altimetry measurements of sea waves continue to be treated as point-wise, static data. Wave period and near surface wind speed are retrieved from the data with statistical methods. However all the parametric models lead us to the most probable values for a given combination of directly measured wave height H_s and normalized radar cross-section σ_0. Thus valuable information of the evolution of wave field along the satellite track is not used. The idea to convert along-track records of the directly measured wave height H_s into unavailable parameters of wind-sea coupling looks promising. The above mentioned estimates of large-scale currents by altimetry methods provide an encouraging example and useful physical analogy.

This analogy is not straightforward as we discussed

the issue above. Dynamical method for large-scale currents is based on reduction of primitive equations of geophysical hydrodynamics when a number of terms are assumed to be small. Negligibility of these terms can be formulated explicitly (e.g. as a smallness of the Rossby number). It is not the case of the model see B14, sect. 2.3. Firstly, this model is based on a number of assumptions and hypotheses of statistical theory of wind-driven seas: evolution of the wave field should be slow enough on scales of wave periods (wave lengths). Secondly, nonlinear transfer should be a dominating term in the Hasselmann equation for simple linking of total (integral) wave input and instantaneous sea state [*Badulin et al.,* 2007; *Zakharov and Badulin,* 2011. Finally, altimetry measurements (the footprint and intervals between consecutive soundings) should provide observability of the above physical link.

The existence of the physical link and subsequent converting of along-track records into sea state parameters implies instantaneous values in contrast to the most probable assessment by parametric models. This is an important point that shows promising prospects for extending our analysis of the altimetry data. The model B14 does not pretend to check or replace the previously proposed methods but does provide additional

information. The combination of the parametric [e.g. G03] and physical B14 models make a ground for advanced wave climatology where mean (the most probable) parameters of the sea state can be extended by estimates of their variations.

The key dimensionless parameter of wave dynamics – wave steepness is used extensively in this work. First, it appears as a result of remarkably simple conversion (2) of the measured along-track variations of wave height into essential information on instantaneous sea state (wave steepness and period). Secondly, we propose to extend the conventional wave climatology by this parameter. Global spatial distributions of this value are presented for the first time, in authors' knowledge. These distributions discover an intriguing feature of wave steepness: its geographical climatic variability is remarkably low in contrast to conventional wave parameters (wave height and period) that show pronounced regional (first of all, latitudinal) dependence. This universality looks promising though it requires further thorough analysis.

Simulations of wave field evolution with state-of-the-art third generation spectral models (WaveWatch III, WAM etc.) can be used in order to verify results presented above. These models demonstrate reasonable

performance in reproducing sea state across the globe. At the same time, the model application at scales of the altimetry measurements when spatial and temporal scaling should follow strict physical constraints, requires additional tuning of the model configurations. Verification of the results of this work within the spectral wave models is a necessary further steps.

5 Conclusions

We summarize the paper by brief overview of its key points.

1. New physical model of wave steepness is designed in order to expand the applications of altimetry data. The model implements the method previously used for the assessment of large-scale currents from altimetry based on geostrophic balance. Both of these approaches are based on the use of spatial gradients of measurable sea state parameters as an extension or/and an alternative to conventional point-wise characteristics H_s, σ_0 of satellite altimetry. The gradient of significant wave height H_s can only be partially estimated as an along-track derivative and thus the routine along-

track altimetry measurements tend to underestimate wave steepness values. The essentially nonlinear dependence (2) makes these estimates acceptable for wave studies. The results are supported by data analysis of buoy-altimeter match-ups and crossover points of altimeters that demonstrates the relevance of the physical model B14 itself and the applicability of the single-track estimates;

2. The proposed physical model does not contain any empirical parameters and therefore does not necessarily need to go through calibration. At the same time the model requires a correspondence on a number of physical scales. The analysis of standard 1-second altimetry data reveals consistency between these scales and those of the today Ku-band altimeters. It is important to point out that this does not guarantee the general applicability of this method, for example, for prospective Ku-band altimeters (e.g. SARAL/AltiKa) due to possible issues with fitting the scaling (8). We consider a good agreement with the standard Ku-band altimetry data with a certain caution and look forward to analyze the implication of this method to different physical scales and new altimetry data;

3. The transparent physics of the new approach ensure operations with instantaneous values of the estimated sea state parameters (wave steepness and period). This approach is conceptually different from widely-used parametric approaches that operate with the best-fit approximation dependencies and thus provide the most probable estimates for the point-wise measurements of H_s and σ_0. We considered one of these models — G03] as a representative example in order to analyze and specify the discrepancy of two approaches. According to our analysis the suggested methods demonstrate a good agreement for estimated wave steepness and periods PDFs for different satellite missions. At the same time the physical model B14 shows wide distributions of their instantaneous estimates while the parametric G03 clenches them up. The sharpening of the G03 PDFs for T_p and μ as compared to those for B14, (see Figure 4) reflects the probabilistic nature of the parametric approach. The G03 model (as well as other parametric models) looks for the best fit in a sub-space of just two measured parameters in, very likely, wider space of physical arguments that affect wave evolution. For two-dimensional distributions in dimensionless

wave periods $\tilde{T}$ and heights $\tilde{H}$ (see Figure 4g,h) the squeezing can be interpreted as a corruption of inherent features of wind-wave coupling when the wave steepness appears to be close to a constant value;

4. Global spatial distribution of wave steepness for both approaches B14 and G03 has been presented for the first time. This provides a motivation for further discussion on potential incorporation of wave steepness into existing sea wave climatologies. In contrast to other wave parameters a trivial averaging of the wave steepness was shown to conceal essential features of the presented physical approach. More subtle procedures are therefore required to develop the proposed method;

5. The validity of the physical model of wave steepness (2) remains a subject of thorough studies. Along with the issue of validity of the asymptotic model (the so-called split-balance model of wind-driven seas [see *Badulin et al.,* 2005, 2007] our approach implies an additional assumption of quasi-stationarity of the wave field. The time derivative $\partial H_s / \partial t$ should be much less than the convective term $C_g \nabla H_s$ (C_g is wave group velocity) that al-

lows to reduce the problem to a fetch-limited setup. All the model assertions would be validated against the spatial estimates of wave period T_p available from global wave model products such as WAM or Wavewatch. These models show quite reasonable performance in reproducing wave periods across the globe. At the same time, their application to the altimetry measurements requires special solutions when spatial and temporal scaling should follow strict physical constraints of sect.2.3. It makes such verification of our results to be an important point of the authors' agenda.

References

Abdalla, S., L. Cavaleri (2002), Effects of wind variability and variable air density on wave modeling, *J. Geophys. Res.*, *107*, no. C7, p. 17-1–17-17, **Crossref**

Babanin, A. V., Y. P. Soloviev (1998), Field investigation of transformation of the wind wave frequency spectrum with fetch and the stage of development, *J. Phys. Oceanogr.*, *28*, p. 563–576, **Crossref**

Badulin, S. I. (2014), A physical model of sea wave period from altimeter data, *J. Geophys. Res. Oceans*, *119*, p. 856–869, **Crossref**

Badulin, S. I., A. V. Babanin, D. Resio, V. Zakharov (2007), Weakly turbulent laws of wind-wave growth, *J. Fluid Mech.*, *591*, p. 339–378, **Crossref**

Badulin, S. I., A. V. Babanin, D. Resio, V. Zakharov (2008), Numerical verification of weakly turbulent law of wind wave growth, *Proceedings of the IUTAM Symposium held in Moscow, 25–30 August, 2006. Vol. 6 of IUTAM Bookseries. Eds. Borisov, A. V., Kozlov, V. V., Mamaev, I. S., Sokolovskiy, M. A.*, p. 175–190, Springer, Berlin, **Crossref**

Badulin, S. I., A. N. Pushkarev, D. Resio, et al. (2005), Self-similarity of wind-driven seas, *Nonl. Proc. Geophys.*, *12*, p. 891–946, **Crossref**

Badulin, S. I., V. E. Zakharov (2017), Ocean swell within the kinetic equation for water waves, *Nonl. Proc. Geophys.*, *24*, p. 237–253, **Crossref**

Barrick, D., B. Lipa (1985), Analysis and interpretation of altime-

ter sea echo, *Advances in Geophysics*, *27*, p. 60–100, **Crossref**

Brown, G. (1977), The average impulse response of a rough surface and its applications, *IEEE Trans. Antennas Propagat.*, *25 (1)*, p. 67–74, **Crossref**

Cavaleri, L., J.-H. G.-M. Alves, F. Ardhuin, et al. (2007), Wave modelling – the state of the art, *Progr. Ocean.*, *75*, p. 603–674, **Crossref**

Chen, K. S., B. Chapron, R. Ezraty (2002), A global view of swell and wind sea climate in the ocean by satellite altimeter and scatterometer, *J. Atmos. Ocean. Technol.*, *19*, no. 11, p. 1849–1859, **Crossref**

Donelan, M. A., W. J. Pierson Jr. (1987), Radar scattering and equilibrium ranges in wind-generated waves with application to scatterometry, *J. Geophys. Res.*, *92 (C5)*, p. 4971–5029, **Crossref**

Donelan, M., M. Skafel, H. Graber, P. Liu, et al. (1992), On the growth rate of wind-generated waves, *Atmosphere Ocean*, *30*, no. 3, p. 457–478, **Crossref**

Dumont, J. P., V. Rosmorduc, N. Picot, E. Bronner, S. Desai, H. Bonekamp, J. Figa, J. Lillibridge, R. Scharroo (2011), *OSTM/Jason-2 Products Handbook, iss. 1 rev. 8*, 63 pp., CNES, EUMETSAT, JPL, NOAA/NESDIS.

Gagnaire-Renou, E., M. Benoit, S. I. Badulin (2011), On weakly turbulent scaling of wind sea in simulations of fetch-limited growth, *J. Fluid Mech.*, *669*, p. 178–213, **Crossref**

Gavrikov, A. V., M. A. Krinitsky, V. G. Grigorieva (2016), Modification of satellite altimetry database globwave for diagnosis of

sea wave fields, *Oceanology*, *56*, no. 2, p. 301–306, **Crossref**

Glazman, R. (1990), Effects of sea maturity on satellite altimeter measurements, *J. Geophys. Res.*, *95*, no. C3, p. 2857–2870, **Crossref**

Gommenginger, C. P., M. A. Srokosz, P. G. Challenor, P. D. Cotton (2003), Measuring ocean wave period with satellite altimeters: A simple empirical model, *Geophys. Res. Lett.*, *30*, no. 22, p. 2150, **Crossref**

Grigorieva, V. G., S. I. Badulin (2016), Wind wave characteristics based on visual observations and satellite altimetry, *Oceanology*, *56*, no. 1, p. 19–24, **Crossref**

Grigorieva, V., S. Gulev (2008), Extreme waves in visual wave observations by VOS, *Proceedings of the Rogue Waves 2008 Workshop, Eds. Olagnon, M., Prevosto, M.*, p. 41–49, Editions IFREMER, Brest.

Gulev, S., V. Grigorieva, A. Sterl, D. Woolf (2003), Assessment of the reliability of wave observations from voluntary observing ships: Insights from the validation of a global wind wave climatology based on voluntary observing ship data, *J. Geophys. Res.*, *108 (C7)*, p. 3236, **Crossref**

Gulev, S. K., V. G. Grigorieva (2006), Variability of the winter wind waves and swell in the North Atlantic and North Pacific as revealed by the voluntary observing ship data, *Journal of Climate*, *19*, p. 5667–5685, **Crossref**

Hasselmann, K. (1962), On the nonlinear energy transfer in a gravity wave spectrum. Part 1. General theory, *J. Fluid Mech.*, *12*, p. 481–500, **Crossref**

Hasselmann, K., D. B. Ross, P. Müller, W. Sell (1976), A paramet-

ric wave prediction model, *J. Phys. Oceanogr.*, *6*, p. 200–228, **Crossref**

Hsiao, S. V., O. H. Shemdin (1983), Measurements of wind velocity and pressure with a wave follower during MARSEN, *J. Geophys. Res.*, *88 (C14)*, p. 9841–9849, **Crossref**

Hwang, P. A., W. J. Teague, G. A. Jacobs, et al. (1998), A statistical comparison of wind speed, wave height and wave period derived from satellite altimeters and ocean buoys in the Gulf of Mexico region, *J. Geophys. Res.*, *103*, no. 10, p. 10451–10468, **Crossref**

Hwang, P. A., D. W. Wang (2004), Field measurements of duration-limited growth of wind-generated ocean surface waves at young stage of development, *J. Phys. Oceanogr.*, *34*, p. 2316–2326, **Crossref**

Kitaigorodskii, S. A. (1962), Applications of the theory of similarity to the analysis of wind-generated wave motion as a stochastic process, *Bull. Acad. Sci. USSR, Geophys. Ser., Engl. Transl.*, p. 105–117, **Crossref**

Mackay, E. B. L., C. H. Retzler, P. G. Challenor, C. P. Gommenginger (2008), A parametric model for ocean wave period from Ku-band altimeter data, *J. Geophys. Res.*, *113*, p. C03029, **Crossref**

Pierson, W. J., L. A. Moskowitz (1964), A proposed spectral form for fully developed wind seas based on the similarity theory of S. A. Kitaigorodsii, *J. Geophys. Res.*, *69*, p. 5181–5190, **Crossref**

Snodgrass, F. E, G. W. Groves, K. F. Hasselmann, G. R. Miller, W. H. Munk, W. H. Powers (1966), Propagation of ocean swell across the Pacific, *Phil. Trans. Roy. Soc. London*, *259 (1103)*,

p. 431–497, **Crossref**

Toba, Y. (1972), Local balance in the air-sea boundary processes. Part I. On the growth process of wind waves, *J. Oceanogr. Soc. Japan*, *28*, p. 109–121, **Crossref**

Vignudelli, S., A. G. Kostianoy, P. Cipollini, et al. (2011), *Coastal Altimetry*, 588 pp., Springer-Verlag, Berlin, Heidelberg, **Crossref**

Voronovich, A. G. (1976), Propagation of internal and surface gravity waves in the approximation of geometrical optics, *Izv. Atmos. Ocean. Phys.*, *12*, p. 850–857.

Young, I. R., S. Zieger, A. V. Babanin (2011), Global trends in wind speed and wave height, *Science*, *332*, p. 451–455, **Crossref**

Zakharov, V. E. (2010), Energy balance in a wind-driven sea, *Phys. Scr.*, *T142*, p. 1–14, **Crossref**

Zakharov, V. E., S. I. Badulin (2011), On energy balance in wind-driven seas, *Doklady Earth Sciences*, *440 (Part 2)*, p. 1440–1444, **Crossref**

Zakharov, V. E., V. S. Lvov, G. Falkovich (1992), *Kolmogorov spectra of turbulence. Part I*, 263 pp., Springer, Berlin, **Crossref**

Zakharov, V. E., M. M. Zaslavsky (1983), Dependence of wave parameters on the wind velocity, duration of its action and fetch in the weak-turbulence theory of water waves, *Izv. Atmos. Ocean. Phys.*, *19*, no. 4, p. 300–306.